wing causes DJNK-mediated apoptosis (Fig. 4f, h). Because aberrant Dpp signalling in either case is deleterious for normal wing morphogenesis, ablation of cells by apoptosis may be an effective mechanism to restore and maintain the normal process of wing development. Downregulation of the DJNK pathway by Dpp signalling is also essential for distal-tip cell survival in several other appendages in addition to the wing. Loss of distal regions owing to cell death in appendages other than the wing have also been observed in *Drosophila* carrying some alleles of *dpp* or *wg*[21,22]. These phenotypes were enhanced in flies with a reduced dosage of the *puc* gene (data not shown), similar to the phenotype we observed in the wing. On the basis of these results, we propose that the regulation of DJNK-dependent apoptosis by a signal gradient providing proximodistal positional value is a general mechanism in appendage development, and is not restricted to the wing. We believe that the DJNK pathway is required for restoration of proximodistal positional information only when signalling levels are abnormal and that normal wing development may not require DJNK signalling. Thus, the DJNK cascade is latent in normal development, but is activated to provide a system to maintain proper development when normal signalling is distorted. □

Methods

A mutant strain *tkv*^{427}. *tkv*^{427} was once reported to be a hyperactive allele based on the result that its wing-vein phenotype was enhanced by an additional *dpp*$^{+}$ transgene[23]. However, similar phenomena can be observed not only in *tkv*^{427} but also in a wide variety of loss-of-function *tkv* alleles (data not shown). Recently, it was also reported that Tkv represses the expression of Dpp required for vein formation during the pupal stage[24]. Thus, hypomorphs of *tkv* produce abundant amounts of Dpp and show the 'thick veins' phenotype enhanced by *dpp*$^{+}$ transgene.

Construction of a transgenic fly *hep*$^{CA(wing\ trap)}$. MKK7, a mammalian homologue of Hep, is activated by phosphorylation at Ser 271, Thr 275 and Ser 277 (ref. 25). Hence, the corresponding amino-acid residues, Ser 346, Thr 350 and Ser 352 in Hep were all replaced with Asp to generate Hep^{CA}. Among 20 strains of *UAS–hep*^{CA} transgenic flies, one insertion in the third chromosome manifested the wing-notch phenotype without GAL4 drivers with a penetrance of less than 10% (Fig. 2c). Furthermore, because ectopic *puc–lacZ* was expressed in the wing disc of this strain (Fig. 1b), the wing-notch phenotype was presumed to be caused by the enhancer trap of the *UAS–hep*^{CA} transgene. This strain was named *hep*$^{CA(wing\ trap)}$ and used throughout this work.

Acridine-orange staining of the wing disc. Staining was carried out as described[26]. Although apoptotic cell clusters were observed in various genetic backgrounds, these were usually accompanied by somewhat elevated levels of sporadic dying cells throughout the wing disc. It has been reported previously that apoptosis induced in a restricted wing area is typically accompanied by nonautonomous death in adjacent territories[15].

Clonal analysis of Tkv^{CA}-induced cell death in the *AyGAL4* system. The *AyGAL4* system is a transgene fusing the following DNA segments: *Actin5C* promoter–FRT (yeast FLP recombinase target)-transcriptional termination signal–*yellow*$^{+}$–FRT–*GAL4* (ref. 27). Discs were prepared from larvae carrying both the *AyGAL4* and *hsFlp* (yeast *FLP recombinase* gene driven by a heat shock promoter) transgenes. GAL4-expressing clones were induced by heat treatment at 37 °C for 30 min at 48–72 h after egg laying. Staining was carried out at 48 h after heat treatment.

Received 5 January; accepted 20 May 1999.

1. Ip, Y. T. & Davis, R. J. Signal transduction by the c-Jun N-terminal kinase (JNK)—from inflammation to development. *Curr. Opin. Cell Biol.* **10,** 205–219 (1998).
2. Campbell, G., Weaver, T. & Tomlinson, A. Axis specification in the developing *Drosophila* appendage: the role of *wingless*, *decapentaplegic*, and the homeobox gene *aristaless*. *Cell* **74,** 1113–1123 (1993).
3. Zecca, M., Basler, K. & Struhl, G. Direct and long-range action of Wingless morphogen gradient. *Cell* **87,** 833–844 (1996).
4. Nellen, D., Burke, R., Struhl, G. & Basler, K. Direct and long-range action of DPP morphogen gradient. *Cell* **85,** 357–368 (1996).
5. Lecuit, T. *et al.* Two distinct mechanisms for long-range patterning by Decapentaplegic in the *Drosophila* wing. *Nature* **381,** 387–393 (1996).
6. Neumann, C. J. & Cohen, S. Long-range action of Wingless organizes the dorsal-ventral axis of the *Drosophila* wing. *Development,* **124,** 871–880 (1997).
7. Neumann, C. J. & Cohen, S. Morphogens and pattern formation. *BioEssays* **19,** 721–729 (1997).
8. Noselli, S. JNK signalling and morphogenesis in *Drosophila*. *Trends Genet.* **14,** 33–38 (1998).
9. Goberdohan, D. C. I. & Wilson, C. JNK, cytoskeletal regulator and stress response kinase? A *Drosophila* perspective. *BioEssays* **20,** 1009–1019 (1998).
10. Segal, D. & Gelbart, W. M. Shortvein, a new component of the decapentaplegic gene complex in *Drosophila melanogaster*. *Genetics* **109,** 119–143 (1985).
11. Terracol, R. & Lengyel, J. A. The *thick veins* gene of *Drosophila* is required for dorsoventral polarity of the embryo. *Genetics* **138,** 165–178 (1994).
12. Riesgo-Escovar, J. R. & Hafen, E. Common and distinct roles of Dfos and Djun during *Drosophila* development. *Science* **278,** 669–672 (1997).
13. Martín-Blanco, E. *et al. puckered* encodes a phosphatase that mediates a feedback loop regulating JNK activity during dorsal closure in *Drosophila*. *Genes Dev.* **12,** 557–570 (1998).
14. Grimm, S. & Pflugfelder, G. O. Control of the gene *optomotor-blind* in *Drosophila* wing development by *decapentaplegic* and *wingless*. *Science* **271,** 1601–1604 (1996).
15. Milán, M., Campuzano, S. & García-Bellido, A. Developmental parameters of cell death in the wing disc of *Drosophila*. *Proc. Natl Acad. Sci. USA* **94,** 5691–5696 (1997).
16. Kurada, P. & White, K. Ras promotes cell survival in *Drosophila* by downregulating *hid* expression. *Cell* **95,** 319–329 (1998).
17. Bergmann, A., Agapite, J., McCall, K. & Steller, H. The *Drosophila* gene *hid* is a direct molecular target of Ras-dependent survival signaling. *Cell* **95,** 331–341 (1998).
18. Hogan, B. L. M. Bone morphogenetic proteins: multifunctional regulators of vertebrate development. *Genes Dev.* **10,** 1580–1594 (1996).
19. Adachi-Yamada, T. *et al.* p38 mitogen-activated protein kinase can be involved in transforming growth factor-β superfamily signal transduction in *Drosophila* wing morphogenesis. *Mol. Cell. Biol.* **19,** 2322–2329 (1999).
20. Brand, A. H. & Perrimon, N. Targeted gene expression as a means of altering cell fates and generating dominant phenotype. *Development* **118,** 401–415 (1993).
21. Spencer, F. A., Hoffman, F. M. & Gelbart, W. M. Decapentaplegic: a gene complex affecting morphogenesis in *Drosophila melanogaster*. *Cell* **28,** 451–461 (1982).
22. Couso, J. P., Bate, M. & Martínez-Arias, A. A *wingless*-dependent polar coordinate system in *Drosophila* imaginal discs. *Science* **259,** 484–489 (1993).
23. Penton, A. *et al.* Identification of two bone morphogenetic protein type I receptors in *Drosophila* and evidence that Brk25D is a *decapentaplegic* receptor. *Cell* **78,** 239–250 (1994).
24. de Celis, J. F. Expression and function of *decapentaplegic* and *thick veins* during the differentiation of the veins in the *Drosophila* wing. *Development* **124,** 1007–1018 (1997).
25. Holland, P. M., Suzanne, M., Campbell, J. S., Noselli, S. & Cooper, J. A. MKK7 is a stress-activated mitogen-activated protein kinase kinase functionally related to *hemipterous*. *J. Biol. Chem.* **272,** 24994–24998 (1997).
26. Masucci, J. D., Miltenberger, R. J. & Hoffmann, F. M. Pattern-specific expression of the *Drosophila decapentaplegic* gene in imaginal discs is regulated by 3′-cis regulatory elements. *Genes Dev.* **4,** 2011–2023 (1990).
27. Ito, K., Awano, W., Suzuki, K., Hiromi, Y. & Yamamoto, D. The *Drosophila* mushroom body is a quadruple structure of clonal units each of which contains a virtually identical set of neurons and glial cells. *Development* **124,** 761–771 (1997).

Acknowledgements. We thank K. Basler, K. Ekstrom, W. M. Gelbart, Y. Hiromi, Y. H. Inoue, T. Kadowaki, K. Matthews, M. Nakamura, S. Noselli, H. Okano, N. Perrimon, G. O. Pflugfelder, G. Struhl, K. Takahashi, D. Yamamoto and S. Yoshikawa for materials; and K. W. Cho, S. Goto, A. Kuroiwa, M. Lamphier, E. Nishida, M. B. O'Connor, T. Tabata and Y. Tomoyasu for advice on the manuscript. Supported by grants from The Award of Tokai Scholarship Foundation, The Kurata Foundation, The Ministry of Education, Science, Sports and Culture of Japan, and Japan Science and Technology Corporation.

Correspondence and requests for materials should be addressed to T.A.-Y. (e-mail: adachi@bio.nagoya-u.ac.jp).

The *mPer2* gene encodes a functional component of the mammalian circadian clock

Binhai Zheng*, David W. Larkin†, Urs Albrecht‡‖, Zhong Sheng Sun*, Marijke Sage*, Gregor Eichele‡‖, Cheng Chi Lee* & Allan Bradley*§

** Department of Molecular and Human Genetics; † Division of Neuroscience; ‡ Verna and Marrs McLean Department of Biochemistry; and § Howard Hughes Medical Institute, Baylor College of Medicine, One Baylor Plaza, Houston, Texas 77030, USA*

Circadian rhythms are driven by endogenous biological clocks that regulate many biochemical, physiological and behavioural processes in a wide range of life forms[1]. In mammals, there is a master circadian clock in the suprachiasmatic nucleus of the anterior hypothalamus. Three putative mammalian homologues (*mPer1*, *mPer2* and *mPer3*) of the *Drosophila* circadian clock gene *period* (*per*) have been identified[2–8]. The *mPer* genes share a conserved PAS domain (a dimerization domain found in Per, Arnt and Sim) and show a circadian expression pattern in the suprachiasmatic nucleus. To assess the *in vivo* function of *mPer2*, we generated and characterized a deletion mutation in the PAS domain of the mouse *mPer2* gene. Here we show that mice

‖ Present address: Max Planck Institute for Experimental Endocrinology, Feodor-Lynen-Strasse 7, 30625 Hanover, Germany.

homozygous for this mutation display a shorter circadian period followed by a loss of circadian rhythmicity in constant darkness. The mutation also diminishes the oscillating expression of both *mPer1* and *mPer2* in the suprachiasmatic nucleus, indicating that *mPer2* may regulate *mPer1 in vivo*. These data provide evidence that an *mPer* gene functions in the circadian clock, and define *mPer2* as a component of the mammalian circadian oscillator.

The PAS domain is highly conserved in circadian clock genes from a variety of species[9–13]. We designed a replacement vector to delete two exons encoding the most conserved region of mPer2 in comparison with *Drosophila* Per (Fig. 1a). This deletion removes half of PAS B and the entire PAC subdomain[14] and is expected to disrupt the PAS domain. The targeted allele (*mPer2*^{Brdm1}, abbreviated as m) was obtained in AB2.2 embryonic stem cells (derived from an XY 129S7/SvEvBrd-*Hprt*$^{b\text{-}m2}$ embryo, abbreviated as 129 below) (Fig. 1b) and used to generate germline chimaeric mice. Intercrosses between heterozygous (C57BL/6 × 129) F_1 offspring produced homozygous mutants (Fig. 1c) at the expected Mendelian ratio. Homozygous mutants (m/m) were morphologically indistinguishable from their wild-type littermates and both males and females were fertile. Reverse transcription with polymerase chain reaction (RT–PCR) and sequence analysis indicated the presence of a mutant transcript that, if translated, would generate a protein with a deletion of 87 amino acids (Fig. 1d).

To determine whether the mutation altered circadian behaviour,

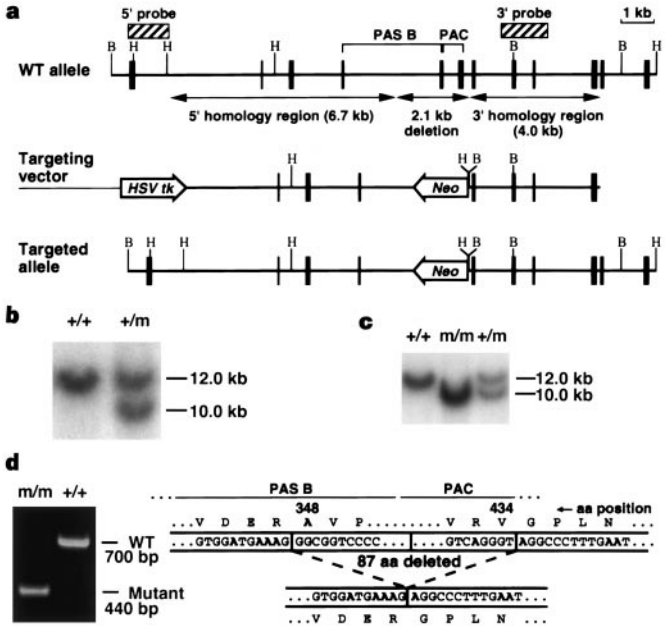

Figure 1 Generation of *mPer2*^{Brdm1} mutant mice. **a**, Genomic structure of a portion of the mouse *mPer2* gene, the targeting vector and the predicted structure of the targeted allele. Exons are indicated by vertical black bars. WT, wild type; H, *Hin*dIII; B, *Bam*HI; *Neo*, neomycin resistance gene; *HSV tk*, Herpes simplex virus thymidine kinase gene. **b**, Southern analysis to identify targeted embryonic stem cell clones by digesting genomic DNA with *Bam*HI. A 1.2-kb 5′ external probe detects a 12.0-kb wild-type (+) fragment and a 10.0-kb mutant (m) fragment. A 1.4-kb 3′ internal probe that detects an 11.2-kb *Hin*dIII wild-type fragment and a 5.7-kb mutant fragment was used to confirm correct targeting at the 3′ homology region (data not shown). **c**, Southern analysis of F_2 littermates obtained from intercrosses between (C57BL/6 × 129) F_1 heterozygous mice using the same restriction enzyme and probe as in **b**. A probe corresponding to the deleted region was used in Southern analysis to confirm the deletion in homozygous mutants (data not shown). **d**, RT-PCR and sequence of the mutant transcripts. Left: RT-PCR products separated on an agarose gel which were amplified with cDNA primers flanking the expected deletion. bp, base pair. Right: comparison of the wild-type and mutant cDNA sequences with conceptual translation shown. Amino-acid position is from GenBank accession number AF036893.

F_2 homozygous mutants and their wild-type and heterozygous littermates were individually housed in circadian activity-monitoring chambers. Wheel-running activity, which is an accurate measure of circadian activity in rodents, was monitored for each animal. Mice were initially maintained in a 12 h light/12 h dark (LD 12:12, or LD) cycle for 10 days to establish entrainment, and were subsequently maintained in constant darkness (DD) (Fig. 2). After 22 days in darkness, the animals were exposed to a 6-h light pulse (arrows in Fig. 2) and were subsequently maintained in darkness for an additional 11 days. F_2 wild-type mice showed a precise entrainment to the LD cycle and in constant darkness they established a circadian rhythm with a period slightly less than 24 h (Fig. 2a). The 6-h light pulse reset the clock of these animals when applied in the subjective night.

Homozygous mutants were also entrained in LD (see below). However, they displayed two overt phenotypes in constant darkness. The first phenotype of homozygous mutants is a short circadian period. At the beginning of DD (Fig. 2b) or after the light pulse (Fig. 2c), homozygous mice typically displayed a short period for several days. The period length was calculated by χ^2 periodogram analyses on intervals when the circadian period appeared stable on the activity record. Wild-type controls had an average period of 23.7 ± 0.4 h (mean ± s.d., $n = 13$). In contrast, m/m mice had an average period of 22.1 ± 0.4 h ($n = 17$), which is 4 s.d. from the mean of the wild-type controls. In some cases the precision of this rhythm in m/m mice could be visualized by replotting the activity record on a scale corresponding to the period (Fig. 2d). The stable period for heterozygous mutants averaged 23.6 ± 0.3 h ($n = 13$), which is not significantly different from that of their wild-type littermates. Thus the homozygous mutants displayed a significantly shorter period than that of their wild-type siblings ($P < 0.001$, Student's t test).

The second phenotype of homozygous mutants is a loss of persistent circadian rhythmicity in constant darkness. The short period expressed by homozygous mutants was followed by a loss of the circadian rhythm (Fig. 2b, c). The time that it took an individual homozygous mutant to lose its circadian rhythm varied, mostly ranging between 2 and 18 days as assessed by activity plots ($n = 17$). None of the wild-type littermates ($n = 13$) became arrhythmic during the corresponding period. Of the heterozygous animals tested ($n = 13$), two displayed multiple rhythms or transient loss of circadian rhythmicity, whereas the other heterozygous mutants were not detectably different from the wild-type controls (data not shown). To quantify circadian rhythmicity, we carried out Fourier periodogram analysis[15] on days 1–10 (the first interval) and days 6–15 (the second interval) in constant darkness for the three genotypes. The logarithm of the amplitude of the circadian peak for the first and second interval averages 2.72 ± 0.14 (mean ± s.e.m.) and 2.80 ± 0.17*, respectively, for +/+ mice ($n = 13$), 2.85 ± 0.08 and 2.88 ± 0.07, respectively, for +/m mice ($n = 13$), and 2.19 ± 0.30 and 1.80 ± 0.35*, respectively, for m/m mice ($n = 17$) (*$P < 0.05$, Student's t test). Fourier analysis on the activity data from homozygous mutants that have no apparent circadian rhythms confirmed the loss of the circadian peak but detected a periodicity of 4–8 h (Fig. 3). Such activity rhythms with a period less than 24 h, known as ultradian rhythms[16], have been observed in rodents with ablated suprachiasmatic nuclei (SCNs)[17], the mouse *Clock* mutant[18] and *Drosophila* clock mutants devoid of circadian rhythms[19]. In contrast, the circadian peak predominated in the wild-type animals and in the mutant animals when they displayed a clear circadian rhythm (Fig. 3a, b and data not shown). Thus the *mPer2*^{Brdm1} mutation provides another example where ultradian rhythmicity can be dissociated from circadian rhythmicity.

The loss of circadian rhythmicity in m/m mice is not due to a decrease in total activity. Total wheel-running activity was not significantly different among the three genotypes in constant darkness (for the first and second interval in DD, wheel rotations per day are 18,849 ± 1,868 and 21,391 ± 2,366, respectively, for +/+ mice,

$n = 13$; 19,833 ± 2,283 and 21,108 ± 2,669, respectively, for +/m mice, $n = 13$; and 20,899 ± 2,402 and 21,708 ± 2,275, respectively, for m/m mice, $n = 17$; numbers are mean ± s.e.m.). The light pulse temporarily restored a circadian rhythm in all m/m animals, which then lasted for a variable period of time (Fig. 2b, c), indicating that the loss of circadian rhythmicity is reversible. Histological analysis of SCN sections showed no gross anatomical difference between +/+ and m/m F_2 littermates (data not shown), indicating that the circadian phenotype in the mutants is not due to a developmental defect in the SCN. To determine whether genetic background affects the expressivity of the circadian phenotype, we generated *mPer2*^{Brdm1} mutants in the 129-inbred strain by crossing chimaeric mice to strain 129 females. The same circadian phenotype was observed in 129-homozygous mutants, that is, a short period for a variable time followed by a loss of circadian rhythmicity (circadian period: +/+, 23.6 ± 0.3 h (mean ± s.d.), $n = 10$; m/m, 22.1 ± 0.5 h, $n = 8$) (for representative activity records, see Supplementary Information, Fig. A). The *mPer2*^{Brdm1} mutation has disrupted two basic properties of the circadian clock, period length and persistence of circadian rhythmicity, showing that *mPer2* functions in the mammalian circadian clock.

Although homozygous *mPer2*^{Brdm1} mutants entrained to the LD cycle, they showed increased locomotor activity in a several-hour period preceding the light-to-dark transition (pre-dusk activity) (Fig. 2c). On average, for F_2 homozygous mutants, 12 ± 1.4% ($n = 17$, mean ± s.e.m.) of the total activity was between ZT 9 and ZT 12. (ZT, zeitgeber time. In an LD 12:12 cycle, light is turned on at ZT 0 and off at ZT 12.) In contrast, wild-type littermates displayed just 2 ± 1.0% ($n = 13$) of their total activity during the same period. Such elevated pre-dusk activity was also observed in 129-homozygous mutants (Supplementary Information, Fig. A). Elevated pre-dusk activity essentially reflects a phase advance in daily activity, which is an expected feature associated with a short period[20,21].

To determine whether the mutation also affects the expression of genes that are believed to be components of the circadian system, we examined the expression of *mPer1*, *mPer2*, *mPer3* and *Clock* in the SCNs of +/+ and m/m littermates, at four different times in the LD cycle, by *in situ* hybridization. Expression of *mPer2* in wild-type controls peaks at around ZT 12 (Fig. 4a), as previously observed[4]. In contrast, *mPer2* transcript levels are much lower at ZT 12 in m/m animals (about 20–40% of wild-type levels by silver grain counting). *mPer2* expression at ZT 6, 18 and 24 is at background levels in the mutants, similar to the wild-type controls. Examination of *mPer2* expression every two hours between ZT 6 and ZT 14 indicated that an overall decrease in expression levels is accompanied by a slight phase advance of transcript oscillation in the mutants (with the new peak of expression at ZT 10; see Supplementary Information, Fig. B). The slight phase advance in *mPer2* expression is consistent with a slight phase advance in the daily rhythm. A similar relationship between behavioural and molecular alterations has been documented in *Drosophila per*^{S} mutants[20,22]. The concordance of the phase shift in circadian activity and transcript oscillation is an expected feature for an oscillator component that describes the progression of the clock[23]. The fact that *mPer2* mutant transcripts still oscillate in the *mPer2*^{Brdm1} mutant SCN in LD indicates that *mPer2* is not solely responsible for its own oscillating expression.

Expression of *mPer1* in the SCN of wild-type littermates is strong at ZT 6 and declines to background levels at ZT 12, 18 and 24, as previously observed[2]. In contrast, *mPer1* expression in the mutants is significantly reduced at ZT 6 (10–30% of wild-type control) (Fig. 4a). At ZT 12, 18 and 24, *mPer1* transcripts are at background levels in the mutants, similar to the wild-type controls. In heterozygous mutants, the expression of *mPer1* or *mPer2* is not detectably different from that in the wild-type controls (Supplementary Information, Fig. C, and data not shown). The constitutive expression of *mPer1* and *mPer2* in the hippocampus and piriform cortex[2,4]

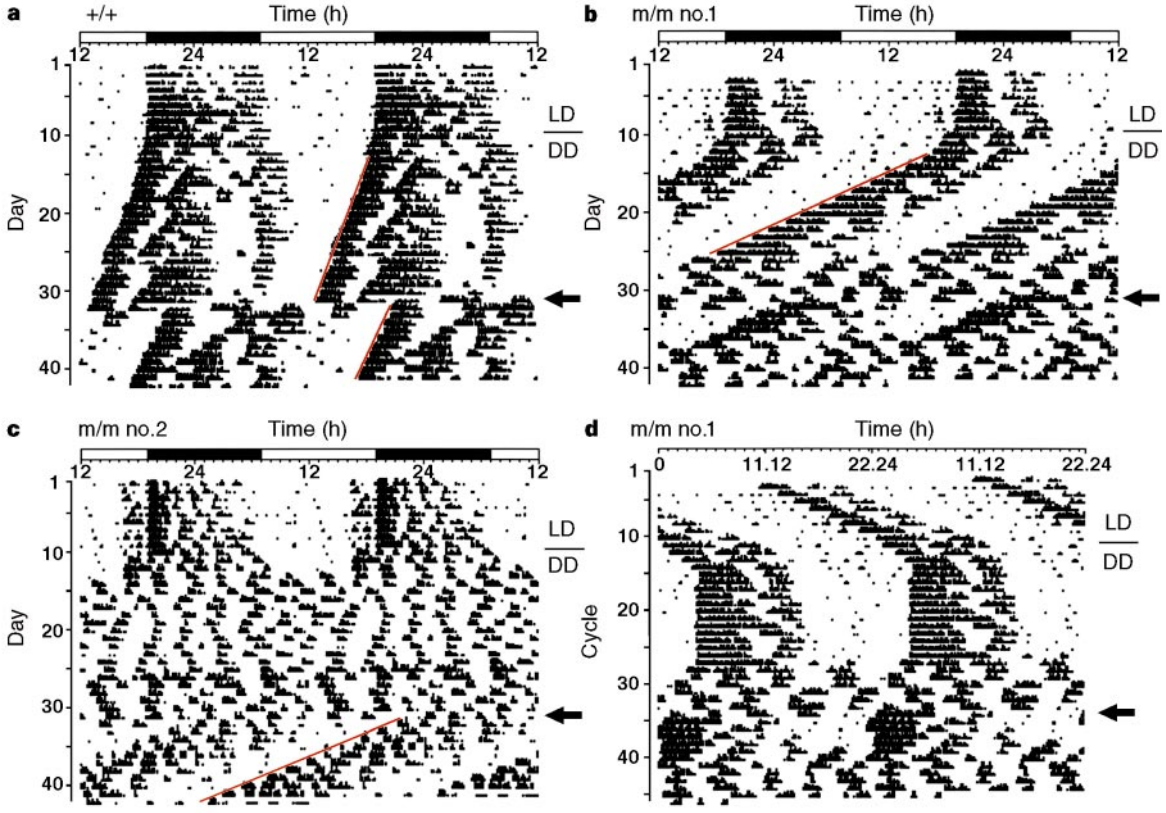

Figure 2 Representative locomotor activity records of F_2 wild-type and homozygous *mPer2*^{Brdm1} mutant mice. Activity records of a wild-type mouse (**a**) and two homozygous mutants (**b**, **c**) are shown. The bar over the records indicates the LD cycle. The line over DD indicates the transition from LD to DD. A 6-h light pulse was applied between 6 pm and midnight (arrow). The slope of the line (in red) aligned with the points of the onset of activity on a 24-h scale plot reflects the period length. **d**, The same activity record as in (**b**) but plotted on a scale corresponding to the period length of this mutant animal.

was not detectably different between +/+ and m/m littermates (Supplementary Information, Fig. D), indicating that the alteration of *mPer1* and *mPer2* expression in the mutant SCN is specific to the rhythmic control of the two genes. In peripheral tissues such as liver and kidney, where *mPer* transcript levels also oscillate strongly[7,24], there was a similar substantial reduction in the amplitude of *mPer1* and *mPer2* transcript oscillation in homozygous *mPer2*^{Brdm1} mutants (Fig. 4b and data not shown). Examination of *mPer1* and *mPer2* expression in the SCN in constant darkness (as assayed every three hours for a 24 h period in the second day in DD) showed a similar reduction of the oscillating expression of the two genes in the mutant as in LD (data not shown).

The *mPer2*^{Brdm1} mutation greatly reduces the rhythmic expression of *mPer1* and *mPer2*, indicating that *mPer2* regulates *mPer1 in vivo*. This implies that *mPer2* is upstream of *mPer1*. It is equally possible that the two genes auto- and cross-regulate in a single molecular cycle for circadian regulation. The reduced expression of *mPer1* and *mPer2* in the mutants, rather than elevated expression, is unexpected given the proposed role of the mPers as negative elements in a putative molecular autoregulatory loop[25]. Instead, our data indicate that mPer2 has positive regulatory functions in the clock, reminiscent of a recent study where *Drosophila* (d)Per was implicated in positive regulation of *dClock*[26]. In contrast to the altered *mPer1* and *mPer2* expression, the expression of both *mPer3* and *Clock* was indistinguishable in the mutant SCN from that of the wild-type controls, and did not appear to oscillate at the four time points sampled in both genotypes (Fig. 4a). Therefore, the alteration of *mPer1* or *mPer2* expression by the *mPer2*^{Brdm1} mutation does not appear to work through a change in either *Clock* or *mPer3* expression.

The phenotype of our deletion mutation underscores the functional importance of the PAS domain of *mPer2*. Given the significant down-regulation of *mPer1* in the SCN of homozygous mutants, the apparently normal *mPer1* expression in the SCN of heterozygous mutants together with a recessive circadian phenotype is consistent with *mPer2*^{Brdm1} being a loss-of-function mutation. However, it is possible that the *mPer2*^{Brdm1} allele has some residual function.

In conclusion, our data show that *mPer2* encodes a dedicated component of the mammalian circadian clock. Given its cyclic expression in the SCN[4–6], our data implicate *mPer2* as an oscillator component of the clock. mPer2 is probably a central clock component, as mutation in *mPer2* leads to a change in the expression of other genes believed to be associated with the clock (*mPer1*). The circadian rhythm in *mPer2*^{Brdm1} mutants is not lost instantly upon release into constant darkness. Rather, the clock continues to operate for a variable period of time and then collapses. A similar feature has been observed in the mouse *Clock* mutant[18]. This characteristic may imply some partial redundancy in the maintenance

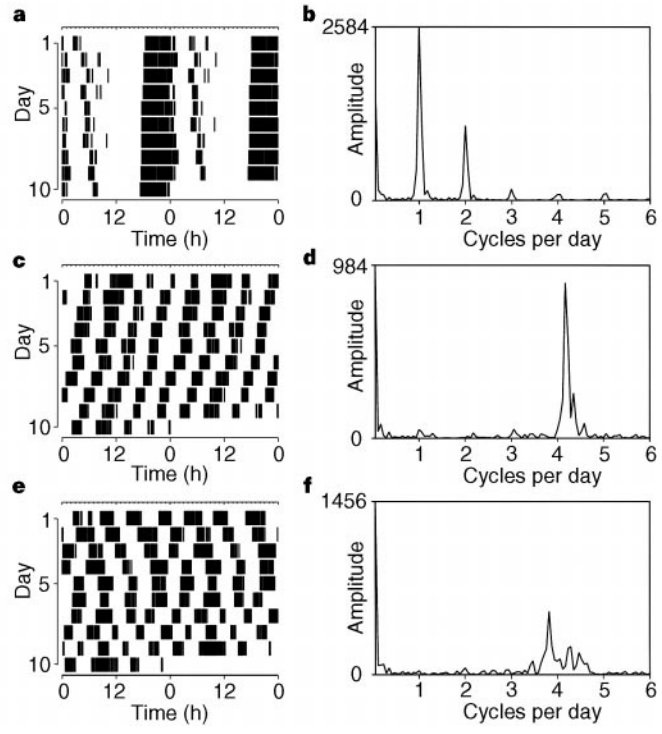

Figure 3 Fourier analysis of periodicity of F_2 wild-type and homozygous *mPer2*^{Brdm1} mutants. Activity records of one wild-type (**a**) and two m/m mice (**c**, **e**) for a 10-day interval in DD, the latter two with no apparent circadian rhythmicity. **b**, **d**, **f**, Fourier periodogram analyses on the activity data plotted in **a**, **c** and **e**, respectively. The amplitude of any rhythm (*y*-axis) is plotted against the number of cycles per day (*x*-axis) with long periods (fewer cycles per day) to the left and short periods (more cycles per day) to the right. A peak at around 1 cycle per day indicates the presence of a circadian rhythm (as in **b**).

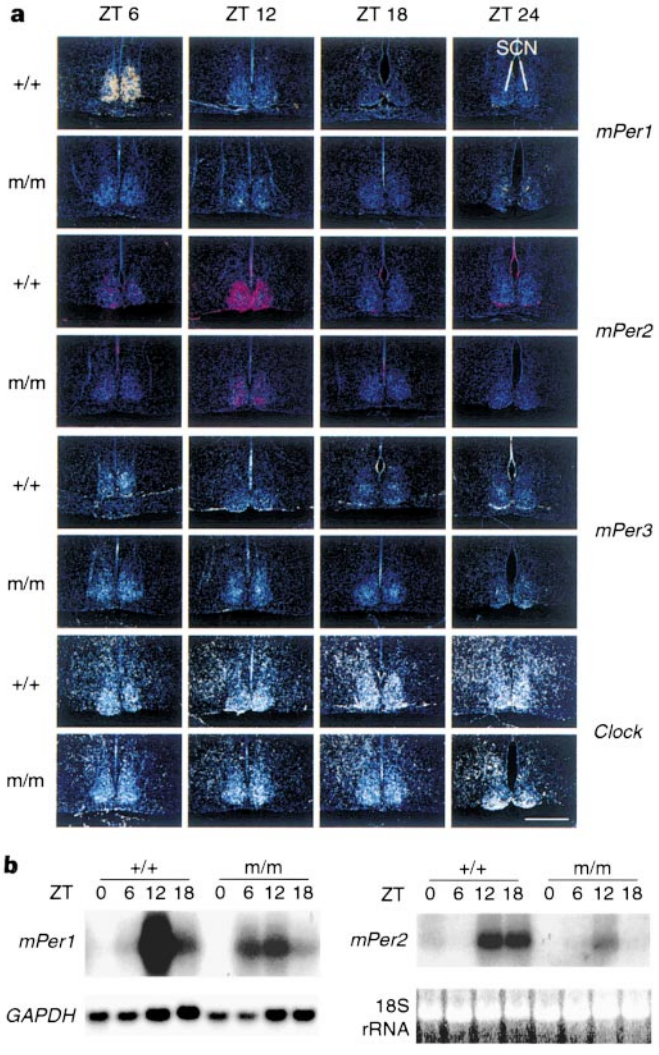

Figure 4 Expression analysis of F_2 wild-type and homozygous *mPer2*^{Brdm1} mutant mice in LD 12:12. **a**, *In situ* hybridization results on SCN of wild-type (+/+) and homozygous mutant (m/m) mice at four different time points. The probes are indicated on the right. Yellow, *mPer1*; red, *mPer2*; white, *mPer3* or *Clock*. Scale bar, 500 μm. **b**, Northern blot analyses of *mPer1* and *mPer2* in liver tissues in +/+ and m/m mice. Duplicate blots were hybridized with a full-length *mPer1* cDNA and a full-length *mPer2* cDNA probe respectively. Re-probing of the same blot with a *GAPDH* probe or ethidium bromide staining of 18S ribosomal RNA was used to control for loading and RNA integrity. Representative results are shown from one out of three independent experiments with similar results, each performed on a different set of animals.

of the circadian cycle in mammals. Mutational analyses of other putative clock genes will be essential for unravelling the molecular mechanisms underlying the mammalian circadian clock. These mutants will also provide useful animal models for elucidating the aetiology of and developing treatments for disorders in humans related to the sleep–wake cycle. □

Methods

Generation of *mPer2*^{Brdm1} mutant mice. We isolated a genomic clone from a mouse 129S5/SvEvBrd genomic library using a mouse *mPer2* complementary DNA probe. A targeting vector was constructed with *PGK-Neo* as the positive selection marker and *HSVtk* as the negative selection marker to delete a 2.1-kilobase (kb) fragment. We used a 6.7-kb *Bgl*II fragment as the 5′ homology region and a 4.0-kb *Kpn*I fragment as the 3′ homology region. The *HSVtk*, *PGK-Neo* and vector backbone were from pKO SelectTK, pKO SelectNeo V800 and pKO Scrambler V924 (Lexicon Genetics). Tissue culture, electroporation, mini-Southern blot analysis on embryonic stem cell colonies, generation of chimaeric and germline mice and tail DNA genotyping were done as described[27,28].

Locomotor activity monitoring and circadian phenotype analysis. Mice were housed in individual cages equipped with a running wheel in ventilated, light-tight chambers with controlled lighting. Wheel-running activity was monitored by an on-line PC using the Chronobiology Kit (Stanford Software Systems). In the LD cycle, the light was turned on at 7:00 (ZT 0) and off at 19:00 (ZT 12). The switch into constant darkness (DD) was effected by not turning on the light at the usual time. The activity records are double plotted so that each day/cycle's activity is shown both to the right and below that of the previous day/cycle. Activity is plotted in density percentile distribution (Fig. 2) or threshold (Fig. 3) format. For activity counting we used the ACTCNT program of the Chronobiology Kit. To determine the period length, an interval with a 10-day minimum during which the circadian period appeared to be stable on the activity record was analysed with a χ^2 periodogram[29] using the Stanford Chronobiology Kit. We used Fourier periodogram analysis[15] in the Chronobiology Kit to assess the strength of circadian and/or ultradian rhythmicity.

***In situ* hybridization.** Mice were killed by cervical dislocation under ambient light conditions at ZT 6 and ZT 12 and under a 15 W safety red light at ZT 18 and ZT 0/24. Specimen preparation and *in situ* hybridization with an *mPer1* and an *mPer2* probe were carried out as described[4,30]. The *mPer2* probe is outside the region deleted in the mutant. The *mPer3* probe was made from an RT–PCR product corresponding to nucleotides 480–824 (AF050182). The *Clock* probe was made from an RT–PCR product corresponding to nucleotides 1352–2080 (AF000998). Tissue was visualized by fluorescence of Hoechst dye-stained nuclei (blue in Fig. 4).

Northern blot and RT-PCR analysis. Tissues were collected and frozen in liquid nitrogen and stored at −80 °C. RNA was prepared with the RNAzol™ B RNA isolation kit (TEL-TEST). We performed northern blot analysis on total tissue RNA using denaturing formaldehyde gel. For RT–PCR analysis, first strand cDNA was generated using Moloney reverse transcriptase (BRL-GIBCO) and oligo dT-priming from total liver RNA. An aliquot of the first strand cDNA was then amplified by PCR across the deletion region with the 5′ primer CTA CCT GGT CAA GGT GCA AGA G and the 3′ primer GGT TTG AAT CTT GCC ACT GG. The RT–PCR products were then sequenced with an internal primer AGG GTA CAC TCG GGC TAT GA.

Received 31 December 1998; accepted 18 May 1999.

1. Pittendrigh, C. S. Temporal organization: reflections of a Darwinian clock-watcher. *Annu. Rev. Physiol.* **55,** 16–54 (1993).
2. Sun, Z. S. *et al. RIGUI*, a putative mammalian ortholog of the *Drosophila period* gene. *Cell* **90,** 1003–1011 (1997).
3. Tei, H. *et al.* Circadian oscillation of a mammalian homologue of the *Drosophila period* gene. *Nature* **389,** 512–516 (1997).
4. Albrecht, U., Sun, Z. S., Eichele, G. & Lee, C. C. A differential response of two putative mammalian circadian regulators, *mper1* and *mper2*, to light. *Cell* **91,** 1055–1064 (1997).
5. Shearman, L. P., Zylka, M. J., Weaver, D. R., Kolakowski, L. F. Jr & Reppert, S. M. Two *period* homologs: circadian expression and photic regulation in the suprachiasmatic nuclei. *Neuron* **19,** 1261–1269 (1997).
6. Takumi, T. *et al.* A new mammalian *period* gene predominantly expressed in the suprachiasmatic nucleus. *Genes Cells* **3,** 167–176 (1998).
7. Zylka, M. J., Shearman, L. P., Weaver, D. R. & Reppert, S. M. Three *period* homologs in mammals: differential light responses in the suprachiasmatic circadian clock and oscillating transcripts outside of brain. *Neuron* **20,** 1103–1110 (1998).
8. Takumi, T. *et al.* A light-independent oscillatory gene *mPer3* in mouse SCN and OVLT. *EMBO J.* **17,** 4753–4759 (1998).
9. Huang, Z. J., Edery, I. & Rosbash, M. PAS is a dimerization domain common to *Drosophila* Period and several transcription factors. *Nature* **364,** 259–262 (1993).
10. Crosthwaite, S. K., Dunlap, J. C. & Loros, J. J. *Neurospora wc-1* and *wc-2*: transcription, photo-responses, and the origins of circadian rhythmicity. *Science* **276,** 763–769 (1997).
11. King, D. P. *et al.* Positional cloning of the mouse circadian *Clock* gene. *Cell* **89,** 641–653 (1997).
12. Rutila, J. E. *et al.* CYCLE is a second bHLH-PAS clock protein essential for circadian rhythmicity and transcription of *Drosophila period* and *timeless*. *Cell* **93,** 805–814 (1998).
13. Allada, R., White, N. E., So, W. V., Hall, J. C. & Rosbash, M. A mutant *Drosophila* homolog of mammalian *Clock* disrupts circadian rhythms and transcription of *period* and *timeless*. *Cell* **93,** 791–804 (1998).
14. Ponting, C. P. & Aravind, L. PAS: a multifunctional domain family comes to light. *Curr. Biol.* **7,** R674–R677 (1997).
15. Bracewell, R. N. *The Hartley Transform* (Oxford Univ. Press, New York, 1986).
16. Aschoff, J. in *Handbook of Behavioral Neurobiology 4: Biological Rhythms* (ed. Aschoff, J.) 3–10 (Plenum, New York, 1981).
17. Ibuka, N., Inouye, S. I. & Kawamura, H. Analysis of sleep-wakefulness rhythms in male rats after suprachiasmatic nucleus lesions and ocular enucleation. *Brain Res.* **122,** 33–47 (1977).
18. Vitaterna, M. H. *et al.* Mutagenesis and mapping of a mouse gene, *Clock*, essential for circadian behavior. *Science* **264,** 719–725 (1994).
19. Dowse, H. B. & Ringo, J. M. Further evidence that the circadian clock in *Drosophila* is a population of coupled ultradian oscillators. *J. Biol. Rhythms* **2,** 65–76 (1987).
20. Hamblen-Coyle, M. J., Wheeler, D. A., Rutila, J. E., Rosbash, M. & Hall, J. C. Behavior of period-altered rhythm mutants of *Drosophila* in light:dark cycles. *J. Insect Behav.* **5,** 417–446 (1992).
21. Ralph, M. R. & Menaker, M. A mutation of the circadian system in golden hamsters. *Science* **241,** 1225–1227 (1988).
22. Hardin, P. E., Hall, J. C. & Rosbash, M. Feedback of the *Drosophila period* gene product on circadian cycling of its messenger RNA levels. *Nature* **343,** 536–540 (1990).
23. Dunlap, J. C. Genetics and molecular analysis of circadian rhythms. *Annu. Rev. Genet.* **30,** 579–601 (1996).
24. Balsalobre, A., Damiola, F. & Schibler, U. A serum shock induces circadian gene expression in mammalian tissue culture cells. *Cell* **93,** 929–937 (1998).
25. Sangoram, A. M. *et al.* Mammalian circadian autoregulatory loop: A *Timeless* ortholog and *mPer1* interact and negatively regulate CLOCK-BMAL1-induced transcription. *Neuron* **21,** 1101–1113 (1998).
26. Bae, K., Lee, C., Sidote, D., Chuang, K. Y. & Edery, I. Circadian regulation of a *Drosophila* homolog of the mammalian *Clock* gene: PER and TIM fucntion as positive regulators. *Mol. Cell. Biol.* **18,** 6142–6151 (1998).
27. Matzuk, M. M., Finegold, M. J., Su, J. G., Hsueh, A. J. & Bradley, A. Alpha-inhibin is a tumour-suppressor gene with gonadal specificity in mice. *Nature* **360,** 313–319 (1992).
28. Ramirez-Solis, R., Davis, A. C. & Bradley, A. Gene targeting in embryonic stem cells. *Methods Enzymol.* **225,** 855–878 (1993).
29. Sokolove, P. G. & Bushell, W. N. The chi square periodogram: its utility for analysis of circadian rhythms. *J. Theor. Biol.* **72,** 131–160 (1978).
30. Albrecht, U., Eichele, G., Helms, J. A. & Lu, H. in *Molecular and Cellular Methods in Developmental Toxicology* (ed. Daston, G. P.) 23–48 (CRC Press, Boca Raton, FL, 1997).

Supplementary information is available on *Nature*'s World-Wide Web site (http://www.nature.com) or as paper copy from the London editorial office of *Nature*.

Acknowledgements. We thank S. Vaishnav, L. Qiu, Y.-C. Cheah, E. Sheppeard and S. Rivera for technical assistance; P. Hastings for comments on the manuscript; J. W. Patrick for providing space and facilities for circadian phenotype analysis; and J. Takahashi, Y. Zhao and M. Bucan for helpful discussions. This work was supported by grants from NINDS and NIDA to J. W. Patrick, from the Max-Planck Society to G. E., from NIH and the Department of Defense to C.C.L., and from NIH and the Howard Hughes Medical Institute to A.B. A.B. is an investigator with HHMI.

Correspondence and requests for materials should be addressed to C.C.L. (e-mail: ching@bcm.tmc.edu)

Immunization with amyloid-β attenuates Alzheimer-disease-like pathology in the PDAPP mouse

Dale Schenk, Robin Barbour, Whitney Dunn, Grace Gordon, Henry Grajeda, Teresa Guido, Kang Hu, Jiping Huang, Kelly Johnson-Wood, Karen Khan, Dora Kholodenko, Mike Lee, Zhenmei Liao, Ivan Lieberburg, Ruth Motter, Linda Mutter, Ferdie Soriano, George Shopp, Nicki Vasquez, Christopher Vandevert, Shannan Walker, Mark Wogulis, Ted Yednock, Dora Games & Peter Seubert

Elan Pharmaceuticals, 800 Gateway Boulevard, South San Francisco, California 94080, USA

Amyloid-β peptide (Aβ) seems to have a central role in the neuropathology of Alzheimer's disease (AD)[1]. Familial forms of the disease have been linked to mutations in the amyloid precursor protein (APP) and the presenilin genes[2,3]. Disease-linked mutations in these genes result in increased production of the